New Islanding Detection Method for Inverter-Based Distributed Generation Considering Its Switching Frequency

Soo-Hyoung Lee, *Student Member, IEEE*, and Jung-Wook Park, *Senior Member, IEEE*

***Abstract*—Islanding detection is one of the most important issues for the distributed generation (DG) systems connected to an electric power grid. The conventional passive islanding detection methods inherently have a nondetection zone (NDZ), and active islanding detection methods might cause problems with safety, reliability, stability, and power quality on a power system. This paper proposes a passive islanding detection method with the zero NDZ property by considering the switching frequency from an inverter of the DG system. Moreover, the proposed method does not cause any negative effects in the aforementioned problems because it avoids applying the intended changes such as variations of reactive power and/or harmonics, which are required in the active islanding detection methods. Several case studies are carried out to verify that the proposed method can detect the islanding operation within 20 ms, which is less than 150 ms required in a recloser as the shortest mechanical reclosing (delay) time. Moreover, this value satisfies the requirement of 2 s given in IEEE Std. 1547.**

***Index Terms*—Distributed generation (DG), inductance concentration bus, islanding detection, load concentration bus, pulsewidth modulation (PWM) inverter, switching frequency.**

I. Introduction

According to the increased prices of fossil fuels such as oil and natural gas, it is expected that the electric power industry will undergo considerable and rapid change with respect to its structure, operation, planning, and regulation. Moreover, trends in power system planning and operation are being toward maximum utilization of existing infrastructures with tight operating margins due to the new constraints placed by economical, political, and environmental factors. The distributed generation (DG) system is one of the most possible solutions to deal with the aforementioned problems.

The DG is based on the renewable energy sources such as fuel cell, photovoltaic, and wind power, as well as combined heat and power gas turbine, microturbine, etc. The number of DG systems is rapidly increasing, and most of them are connected to a distribution system by supplying power into the network, as well as local loads [1]. An islanding operation occurs when the DG continues supplying power into the network after power from the main utility is interrupted [2], [3]. If the islanding operation occurs, the distribution network becomes out of the utility's control. It can therefore cause a number of negative impacts on the network and DG itself, such as the safety hazards to utility personnel and the public, the power quality problems, and serious damage to the network and DG unless the main utility power is restored correctly and quickly [1]. Furthermore, the DG system must be also disconnected from the network for its protection by the effective detection method before the recloser starts to operate following by the islanding operation.

Two types of islanding detection methods, which are the passive and active methods, have so far been developed. Some representative passive methods detect the islanding operation by monitoring over-/undervoltage (OUV) and over-/underfrequency (OUF) [4], [5]. The changes of voltage and frequency are caused by the mismatches of active and reactive power, respectively. However, these methods have the nondetection zone (NDZ), where the OUV/OUF-based detection method fails to detect the islanding operation. This NDZ is calculated by setting the threshold values for frequency and amplitude of the voltage [6]. In practice, the rate of change of frequency and vector-shift methods are very commonly used in the U.K. and other European countries [7]. Although these methods are effective in reducing the NDZ, they cannot remove it completely. The other passive methods using voltage unbalance (VU) and total harmonic distortion (THD) might determine the islanding operation even in the NDZ [1]. However, those passive methods still neither overcome the NDZ completely nor operate fast enough, despite using the VU and THD methods.

On the other hand, the active method has negative effects on the power system even though it can reduce the NDZ and islanding detection time by injecting harmonics, varying active and reactive powers, or changing grid impedance [3]. In other words, it might cause malfunction in the islanding detection algorithm applied to an inverter-based DG and degrade the voltage stability, power quality, and service reliability [8]. Although the other active methods using supplementary transmitter and receiver have no NDZ, they impose additional costs [9]. The design of the aforementioned anti-islanding algorithm for a

Manuscript received May 14, 2009; revised May 14, 2009 and November 3, 2009; accepted November 23, 2009. Date of publication May 10, 2010; date of current version September 17, 2010. Paper 2009-PSEC-114.R2, presented at the 2009 Industry Applications Society Annual Meeting, Houston, TX, October 4–8, and approved for publication in the IEEE TRANSACTIONS ON INDUSTRY APPLICATIONS by the Power Systems Engineering Committee of the IEEE Industry Applications Society. This work was supported by the Human Resources Development Program of the Korea Institute of Energy Technology Evaluation and Planning (KETEP) grant funded by the Korea Government Ministry of Knowledge Economy (Grant 2007-P-EP-HM-E-08-0000).

The authors are with the School of Electrical and Electronic Engineering, Yonsei University, Seoul 120-749, Korea (e-mail: reasonable@yonsei.ac.kr; jungpark@yonsei.ac.kr).

Digital Object Identifier 10.1109/TIA.2010.2049727

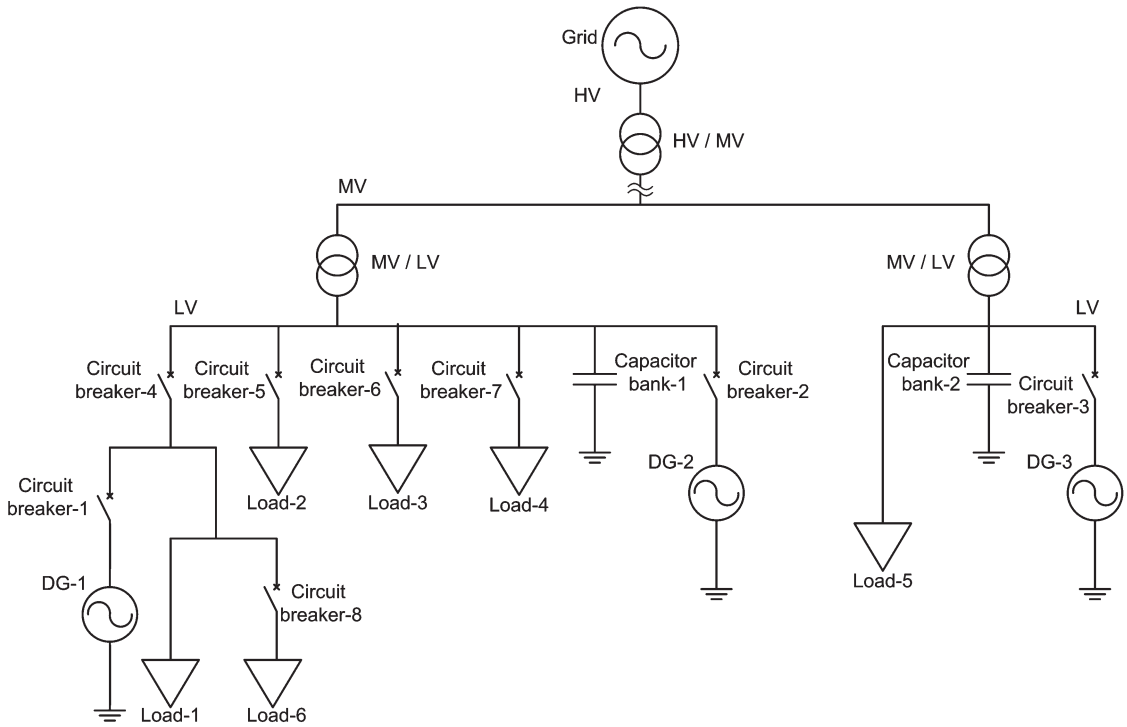

Fig. 1. Distribution power network interconnected with multiple DG systems.

small DG system requires reducing computing efforts [10]. Therefore, the objective of this study is to develop an islanding detection method, which is much faster than the shortest mechanical reclosing (delay) time without extra cost and negative effects.

Generally, the shortest reclosing time is known as 150 ms [6]. This paper makes the new contribution by developing the new passive method to determine the islanding operation within 20 ms based on the switching frequency of inverters.

This paper is organized as follows. Section II describes the proposed islanding detection method based on the switching frequency of a pulsewidth modulation (PWM) inverter. Then, Section III presents the characteristics of impedance at the switching frequency of a single DG system. Several case studies on the distribution power network in Fig. 1 with multiple DG systems are carried out in Section IV to evaluate the performance of the proposed method. Finally, conclusions are given in Section V.

II. Islanding Detection Method Based on Switching Frequency of PWM Inverter

A. NDZ by OUV/OUF Method

After an islanding operation occurs, there might be power mismatch between power generations and load consumptions in the isolated system. Then, it causes changes of voltage and frequency [5], and this islanding operation is detected by monitoring those changes if they are large enough. However, the conventional OUV/OUF passive method has the NDZ, as shown in Fig. 2, where the islanding operation is not detected due to the small changes of voltage and frequency. In Fig. 2, $V_{\min}$, $V_{\max}$, $f_{\min}$, and $f_{\max}$ are the thresholds of under- and overvoltages

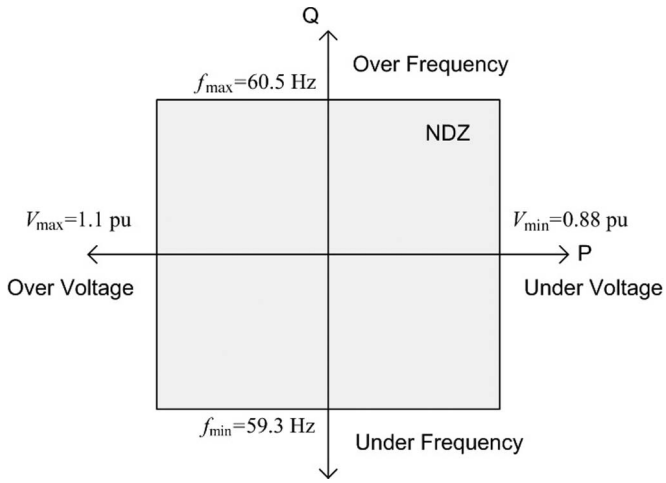

Fig. 2. NDZ by the OUV/OUF-based method.

and under- and overfrequencies, respectively. Those values are typically 0.88 pu, 1.1 pu, 59.3 Hz, and 60.5 Hz, respectively, for each even though these limits are dependent, to some degree, on the interface control design [4].

B. Description of Distribution Power Network

The DG system is usually located on a distribution power network, as shown in Fig. 1, and a capacitor bank is also placed in the network to compensate voltage by supplementing reactive power. To model the distribution system in Fig. 1 in detail, two terms are now defined with the description of bus type. One is the inductance concentration bus, and the other one is the load concentration bus. In the case that a bus has large inductance because it is interconnected with relatively many

TABLE I
SIZES AND PARAMETERS OF ALL DEVICES IN FIG. 1

Component	Real power (kW)	Reactive power (kVAR)	Switching frequency (kHz)
DG-1	15	0	15
DG-2	15	0	16
DG-3	15	0	15
Load-1	15	3	--
Load-2	250	50	--
Load-3	500	100	--
Load-4	250	50	--
Load-5	500	100	--
Load-6	15	3	--
Capacitor bank-1	0	103	--
Capacitor bank-2	0	100	--

distribution lines, it is defined as the inductance concentration bus. For example, the left low voltage (LV) bus in Fig. 1 is considered as the inductance concentration bus when compared to the right LV bus. For its reactive compensation, the capacitor bank is mostly installed on the inductance concentration bus [11]. In a similar manner, the bus interconnected with a large number of loads is defined as the load concentration bus [12]. The left LV bus in Fig. 1 also falls under the load concentration bus because it has relatively large loads. To supply power efficiently, multiple DG systems can be connected to this load concentration bus. The sizes and parameters of all devices in Fig. 1 are given in Table I.

C. Case of Grid-Connected Single DG System

In a real distribution network, the feeder between the high voltage (HV)/medium voltage (MV) and MV/LV transformers in Fig. 1 has large impedance with a similar order of magnitude to the transformer impedance when compared to that of short distribution lines in the LV side. For example, the distribution network in a part of Seoul, Korea, as shown in Fig. 1 (the distribution power system in Fig. 1 is modeled based on the real parameters of this practical network), has many short-line feeders in the LV side with impedance less than 0.05 pu. On the other hand, the associated MV/LV transformer has the impedance of 0.18 pu.

Therefore, the distribution network in Fig. 1 is reformed with the simplified system shown in Fig. 3 to evaluate the effect of the proposed islanding detection method with a single DG connected to an electric power grid based on the PWM inverter. The output of the PWM inverter includes the high-frequency harmonics resulting from its periodic fast switching operation. As mentioned earlier, the high-frequency components from the inverter hardly pass through the transformer since the transformer impedance is much larger than that of the distribution lines in the LV side. This means that high-frequency harmonics over the switching frequency in the voltage and current waveforms measured at the point of common coupling (PCC) in Fig. 3 come only from the inverter, but not from the grid.

The impedances referred to the DG system in Fig. 3 can be estimated from the correspondingly measured voltage and currents [13]. Then, the simplified distribution system in Fig. 3 is modeled with the estimated impedances, as shown in Fig. 4.

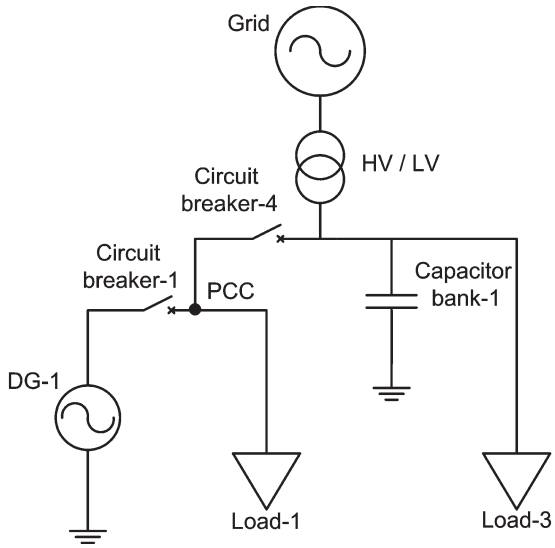

Fig. 3. Simplified distribution network with a single DG system.

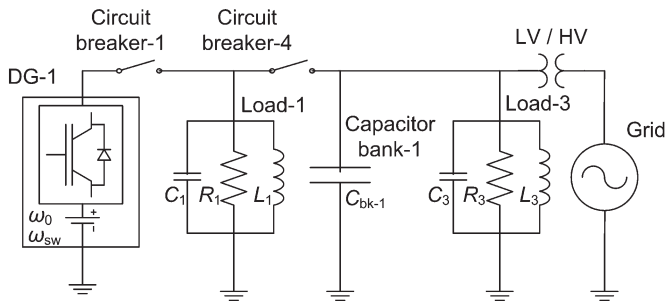

Fig. 4. Modeling of the distribution network with the estimated impedances.

To compare the impedances before and after the islanding operation, the associated parameters are defined as follows:

R_1 resistance of Load-1;
L_1 inductance of Load-1;
C_1 capacitance of Load-1;
R_3 resistance of Load-3;
L_3 inductance of Load-3;
C_3 capacitance of Load-3;
$C_{\text{bk-1}}$ capacitance of Capacitor bank-1;
ω_0 fundamental system frequency;
ω_{sw} switching frequency of the inverter of DG-1.

Again, the impedance of the LV/HV transformer with respect to high frequency is very large when compared to those of Load-1, Load-2, and Capacitor bank-1. Therefore, the impedance of the transformer referred to on the side of DG-1 is negligible for high frequencies over the switching frequency of the inverter when the parallel sum of impedances with Load-3 is considered. Then, the total impedance Z before and after islanding operation by Circuit breaker-4 in Fig. 3 is expressed by (1) and (2), respectively. When the impedances of the feeder in the HV side and the transformer are similar, the LV/HV transformer in Fig. 4 can be removed from the model. Then, its effect on the change in impedances is small for the islanding operation because the total impedance in the right-hand side of Circuit breaker-4 is always much smaller than that of the open circuit. Moreover, the capacitance of the entire feeders does not

affect significantly because it is much smaller than that of the capacitor bank $C_{\text{bk-1}}$

$$Z_{\text{before}} = \frac{1}{\frac{1}{R_1}+\frac{1}{R_3}+j\left(\omega_0 C_1-\frac{1}{\omega_0 L_1}\right)+j\left(\omega_0 C_3+\omega_0 C_{\text{bk-1}}-\frac{1}{\omega_0 L_3}\right)} \quad (1)$$

$$Z_{\text{after}} = \frac{1}{\frac{1}{R_1}+j\left(\omega_0 C_1-\frac{1}{\omega_0 L_1}\right)}. \quad (2)$$

A capacitor bank is mostly installed to compensate voltage, as well as to improve power factor. Assume that all active power required in Load-3 is supplied from the grid. This means that DG-1 also supplies all power to Load-1. When the capacitance of Capacitor bank-1 is given as (3), Load-3 might have close-to-unity power factor because R_3 can be ignored in high-frequency mode

$$C_{\text{bk-1}} = \frac{1}{\omega_0^2 L_3} - C_3. \quad (3)$$

In this case, the overall system voltage and frequency referred to DG-1 do not change because Load-1 has unity power factor, which is the same as that of the inverter output, and the impedances Z_{before} and Z_{after} in (1) and (2) become the same. Therefore, the conventional OUV/OUF passive method cannot detect the islanding operation. In the meanwhile, the switching frequency of the inverter ω_{sw} is given as $\omega_{\text{sw}} = m_f \cdot \omega_0$, where m_f is the frequency modulation. Then, the impedance Z_{sw} with respect to the frequency modulation is calculated by

$$Z_{\text{sw}} = \frac{1}{\frac{1}{R_1}+j\left(m_f\alpha-\frac{\beta}{m_f}\right)} \quad (4)$$

where

$$\alpha = \omega_0(C_1+C_3+C_{\text{bk-1}}) \qquad \beta = \frac{1}{\omega_0}\left(\frac{1}{L_1}+\frac{1}{L_3}\right). \quad (5)$$

Fig. 5 shows the variation of Z_{sw} corresponding to m_f when $L_1 = 0.01$ H, $L_3 = 0.0001$ H, $C_1 = 0.00001$ F, $C_3 = 0.001$ F, and $R_1 = 1\ \Omega$. It is observed that the impedance under the islanding condition is 262 times larger than that under the preislanding condition with the m_f of ten. The m_f of 21–330 is considered in the PWM inverter of the DG system when the usual switching frequency is 1260 Hz–20 kHz [14], [15] for the grid-connected DG systems. Therefore, the islanding operation can be detected perfectly by this variation in impedance with respect to the switching modulation of the inverter.

D. Case of Grid-Connected Multiple DG Systems

Some islanding detection methods [1], [4] use the DG system, which injects harmonic currents based on the THD factor to cancel out the high-frequency harmonics resulting from nonlinear loads. However, when these harmonics are detected on a system with multiple DG systems, it is difficult to know exactly which DG can deal with the undesired harmonics.

The proposed method is not interrupted by the aforementioned case because it operates at much higher frequency than the harmonics from nonlinear sensitive loads. Moreover, the proposed method requires the only particular frequency for each DG system. In other words, it detects the islanding condition clearly only if multiple DG systems are connected to a distribution network with different switching frequencies of their PWM inverter. As described previously, the harmonics corresponding to switching frequencies are highly damped by the transformer due to its large impedance. Therefore, the proposed method can also be applied to the DG systems with even the same switching frequencies if they operate in different areas separated by a transformer. For example, the DG-1/DG-3 and DG-2/DG-3 in Fig. 1 confirm this case.

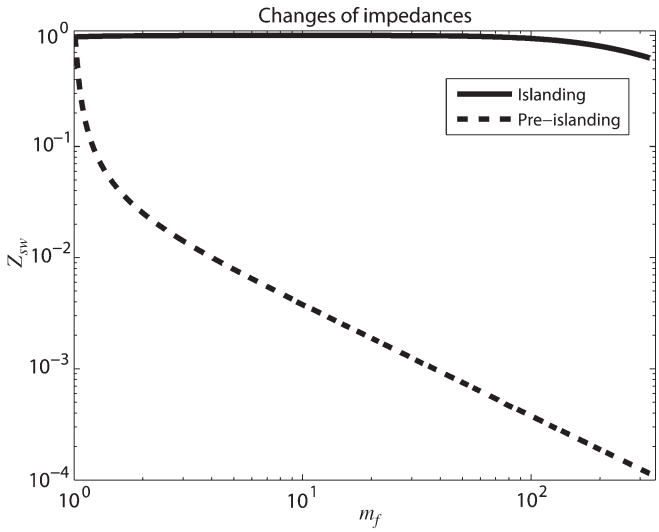

Fig. 5. Variation of the impedance Z_{sw} corresponding to m_f.

E. Implementation of Proposed Detection Method

When the switching frequencies of two DG systems in the same area are very close each other, the signal bandwidth is wide in the frequency domain. For the successful operation of the proposed islanding detection method, it requires making the bandwidth of its frequency response narrow with the longer sampling time. In this case, the improvement of the resolution in the frequency domain based on the fast Fourier transform (FFT) can make the islanding detection time longer than the shortest mechanical reclosing (delay) time required in a recloser. Moreover, the proposed method needs to find the impedance at only one switching frequency. The proposed algorithm is therefore implemented directly in the time domain without the analysis in the frequency domain such as the FFT. This is shown in Fig. 6.

It first generates sine and cosine waveforms with the switching frequency ω_{sw}. They are multiplied individually by the real measurements of the voltage and current at the PCC. Then, their average values during one period T of the waveforms are calculated. The required impedance is finally estimated by the Z_{est} in (6), shown at the bottom of the next page, without direct calculation in (4) with the manipulations of those average values, as shown in Fig. 6. Note that ω_h in $v(\omega_h\tau)$ and $i(\omega_h\tau)$ in (6) indicates each hth harmonic frequency. The average of

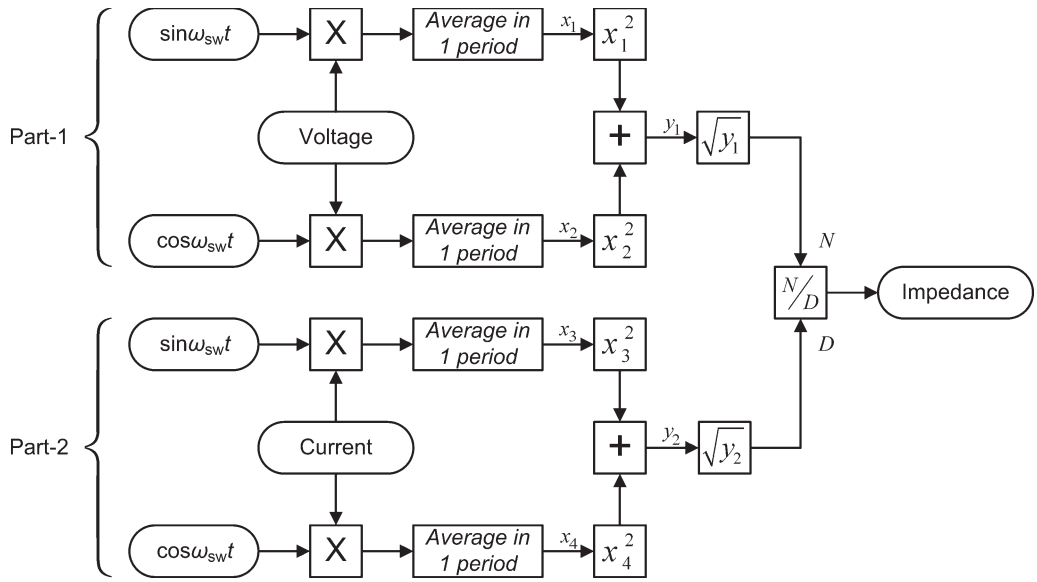

Fig. 6. Implementation of the proposed islanding detection algorithm based on the orthogonal characteristic of high-frequency components.

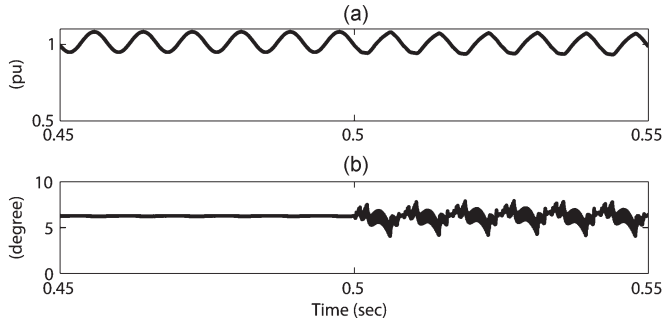

Fig. 7. Responses of the a-phase voltage at the terminal of DG-1 after the islanding operation at 0.5 s. (a) Magnitude. (b) Phase.

two sinusoidal waveform products at different high frequencies is zero because they have the orthogonal characteristic in high-frequency mode. Therefore, the aforementioned implementation with consideration of a particular switching frequency is reasonable.

III. Case Studies in Single DG System

A. Case of Small Difference Between Load Consumption and DG Output Power After Islanding

The case with small difference between single DG system output and load consumption after the islanding operation (by Circuit breaker-4) at 0.5 s is tested using PSCAD/EMTDC simulation on the system in Fig. 3. The result in Fig. 7 shows that the magnitude of the a-phase voltage at the terminal of DG-1 rarely changes. Moreover, its phase response shows small high-frequency perturbations after 0.5 s; therefore, the change of the corresponding system frequency is also small. As mentioned in Section II, the traditional OUV/OUF method fails to detect the required islanding operation in this case because the variations of the aforementioned voltage and phase (frequency) responses are inside the NDZ in Fig. 2.

However, the voltage response corresponding to the high switching frequency of the PWM inverter by the proposed method will show the sudden change after islanding because there is a large difference in the impedance $Z_{\rm sw}$ in (4) between the islanding and preislanding operations, as shown in Fig. 5. The result in Fig. 8 shows the voltage (magnitude) response at the terminal of DG-1 in this particular high-frequency mode (of 1.5 kHz with $m_f = 250$). It suddenly increases right after the islanding occurs. On the other hand, there is no change in the preislanding operation. Therefore, the proposed method determines the islanding operation successfully even in the NDZ, where it cannot be detected by the OUV/OUF method.

B. Case of Large Difference Between Load Consumption and DG Output Power After Islanding

Assume that Load-6 shown in Fig. 1 is connected with Load-1 in Fig. 3 in parallel. This creates a large difference between the DG-1 output and power consumption from Load-1 and Load-6 after islanding. The results in Figs. 9 and 10 show that the OUV/OUF-based method can be possibly used as

$$Z_{\rm est}(t) = \frac{\sqrt{\left(\int_{t_0}^{t_0+T} v(\omega_h\tau)\cdot\sin(\omega_{\rm sw}\tau)\,d\tau\right)^2 + \left(\int_{t_0}^{t_0+T} v(\omega_h\tau)\cdot\cos(\omega_{\rm sw}\tau)\,d\tau\right)^2}}{\sqrt{\left(\int_{t_0}^{t_0+T} i(\omega_h\tau)\cdot\sin(\omega_{\rm sw}\tau)\,d\tau\right)^2 + \left(\int_{t_0}^{t_0+T} i(\omega_h\tau)\cdot\cos(\omega_{\rm sw}\tau)\,d\tau\right)^2}} \tag{6}$$

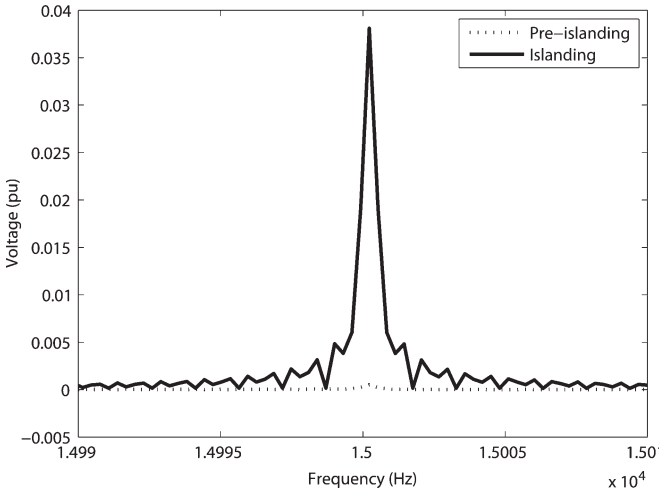

Fig. 8. Voltage response at high switching frequency (15 kHz) of the PWM inverter in the islanding and preislanding operations.

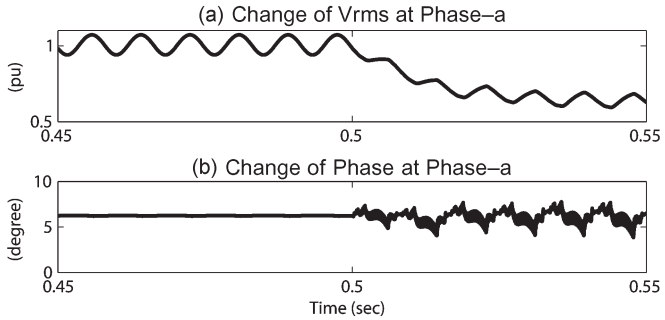

Fig. 9. Responses of the a-phase voltage at the terminal of DG-1 after the islanding operation at 0.5 s. (a) Magnitude. (b) Phase.

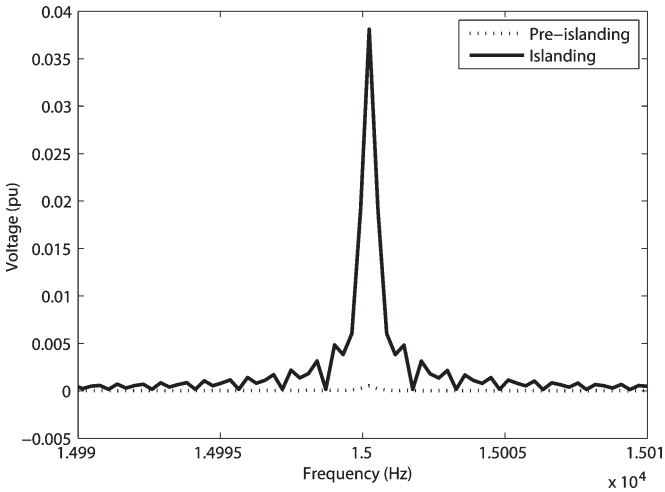

Fig. 10. Voltage response at high switching frequency (15 kHz) of the PWM inverter in the islanding and preislanding operations.

an islanding detection method from its voltage response. In summary, both the OUV/OUF and proposed methods provide the desirable islanding detection performance for this case.

C. Consideration of SNR

To apply the proposed method to a practical system, the effect of noises and measurement errors needs to be analyzed since these undesirable signals might cause to aggravate the signal-to-noise ratio (SNR) problem nearby the switching frequency. The reduced SNR is therefore required at the terminal of DG, where the signals are measured to implement the proposed method.

According to IEEE Std. 1547 in Table II, the voltage harmonics $(35 \leq h)$ corresponding to the switching frequency must be less than 0.3% of the fundamental component. In contrast, the corresponding voltage by the proposed method in Figs. 8 and 10 increases up to about 4% (assume that the terminal voltage of DG is 1 pu) when the islanding operation occurs. This is a remarkable distinction. Moreover, the harmonic noises exist over the entire frequency bands, not at the only particular frequency. Moreover, the effect of measurement errors is similar to that of noise except that it occurs during the measurement processing.

In summary, the magnitude of the switching frequency component caused by the noise and measurement errors is so small than the corresponding response by the proposed method. Therefore, it can be successfully applied to a real distribution system with the DG.

TABLE II
OUTPUT VOLTAGE HARMONICS OF THE DG-1 SYSTEM

	Individual harmonic order					THD
	h<11	11≤h<17	17≤h<23	23≤h<35	35≤h	
IEEE Std. 1547	4.0	2.0	1.5	0.6	0.3	5.0
DG-1	1.41	0.06	0.05	0.06	0.2	1.46

TABLE III
STATES OF THE CIRCUIT BREAKERS TO CARRY OUT SEVEN CASE STUDIES

	Case	Number of circuit breaker							
		1	2	3	4	5	6	7	8
State	A	o	x	x	o→x	o	x	o	o
	B	o	x	x	o→x	o	x	o	x
	C	o	x→o	x	o	o	x	o	x
	D	o	x	x→o	o	o	x	o	x
	E	o	x	x	o	o	x→o	o	x
	F	o	x	x	o	o	x	x→o	x
	G	o	x	x	o→x	o	x	o	x

o: close, x: open, →: change at 0.5 s

IV. CASE STUDIES IN MULTIPLE DG SYSTEMS

It is important to verify whether the proposed islanding detection technique remains robust and has a negligible NDZ on a system with the multiple grid-connected DG systems. A total of seven case studies are carried out on the distribution network with three DG systems in Fig. 1.

Table II shows that the output voltage harmonics of the DG-1 system in the preislanding condition satisfy the requirement of IEEE Std. 1547 for maximum harmonic voltage distortion in percent of the rated voltage. Moreover, seven case studies are implemented by the different operation (called *state*) of the total eight circuit breakers in Fig. 1, as shown in Table III. The

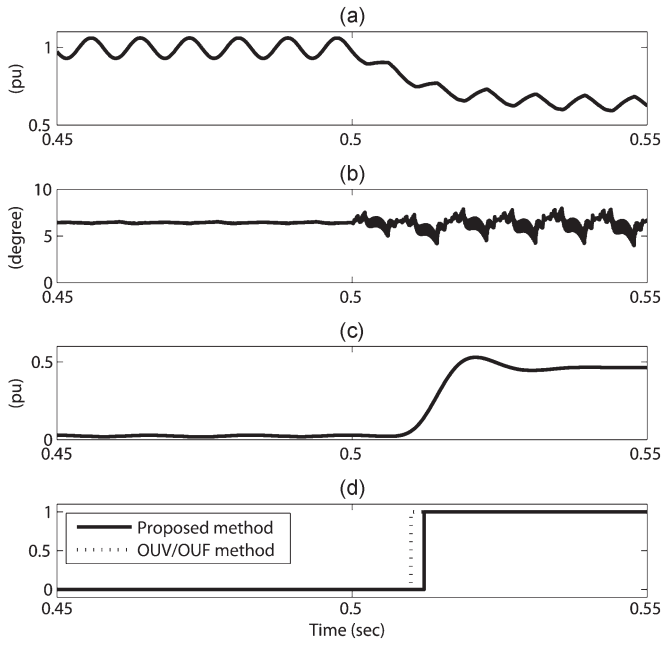

Fig. 11. Responses in case study A. (a) Magnitude of voltage. (b) Phase of voltage. (c) Variation of impedance. (d) Variation of trip signal.

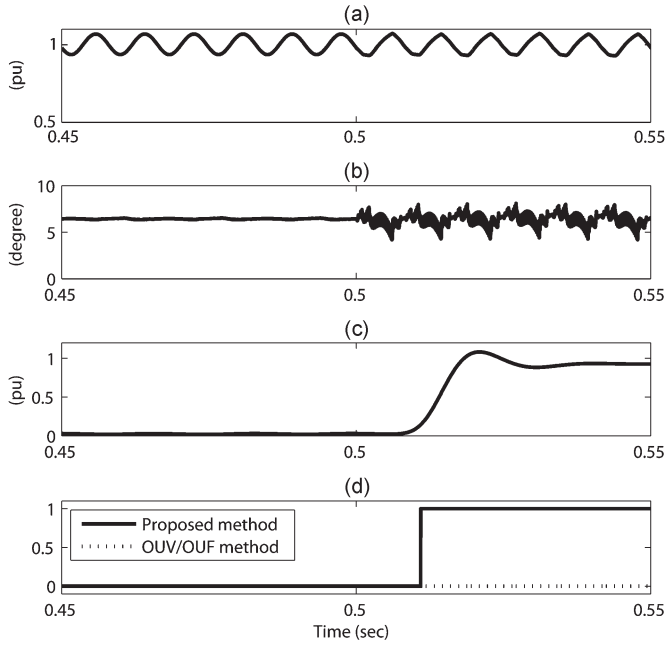

Fig. 12. Responses in case study B. (a) Magnitude of voltage. (b) Phase of voltage. (c) Variation of impedance. (d) Variation of trip signal.

change of this state followed by the islanding detection occurs at 0.5 s in each case.

A. Case of Large Difference Between Load Consumption and DG Output Power After Islanding

The test is carried out by the operation of Circuit breaker-4, which opens at 0.5 s, as shown in Table III. The results are shown in Fig. 11. As in the case study in Section III-B, the islanding operation is easily detected by the conventional OUV/OUF method when the voltage exceeds the threshold of NDZ in Fig. 2 due to the large difference between load consumption and DG-1's output power on the isolated area [see Fig. 11(a)]. Moreover, the proposed method shows good islanding detection performance by its estimated impedance variation, as shown in Fig. 11(c). From the corresponding trip signals in Fig. 11(d), both methods provide fast operation with about 10-ms detection time, which is much shorter than the required shortest reclosing time of 150 ms.

B. Case of Small Difference Between Load Consumption and DG Output Power After Islanding

When the difference between load consumption and DG-1's output power is not large enough, the results are shown in Fig. 12. The change in magnitude of the a-phase voltage at the terminal of DG-1 is very small after 0.5 s [see Fig. 12(a)]. Therefore, the OUV/OUF method fails to detect islanding. In contrast, the results shown in Fig. 12(c) and (d) illustrate that the proposed method still provides successful detection operation without degrading its performance. This independent property on the amount of difference between load consumption and power generation makes the proposed islanding detection technique robust, giving the great benefit of negligible NDZ.

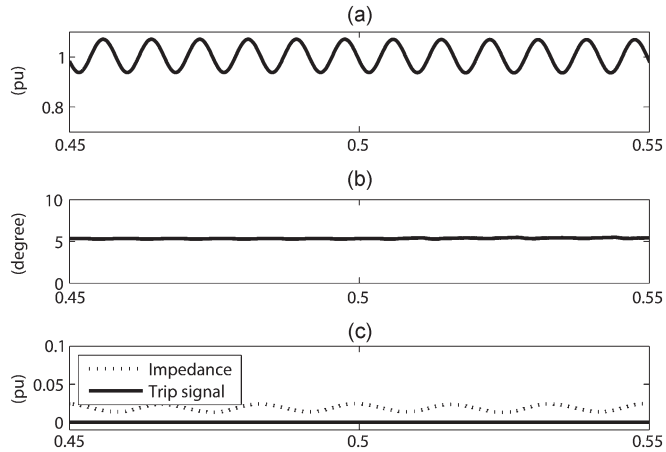

Fig. 13. Responses in case study C. (a) Magnitude of voltage. (b) Phase of voltage. (c) Variation of impedance and trip signal.

C. Connection of Another DG System With Different Switching Frequency

Interaction between multiple DG systems is one of the important and difficult problems which must be solved with careful analysis without regard to active and passive islanding detection methods. This situation is simulated by the operation of Circuit breaker-2 in Fig. 1, which closes at 0.5 s. Then, the islanding detection performance of the proposed method is evaluated by assigning different switching frequencies of 15 and 16 kHz to the DG-1 and DG-2 systems, respectively. Even though there exist active and reactive power mismatches on the system by connecting the DG-2 system, the islanding operation must not occur for this case.

The results are shown in Fig. 13. The proposed method does not misjudge the connection of DG-2 as an islanding operation,

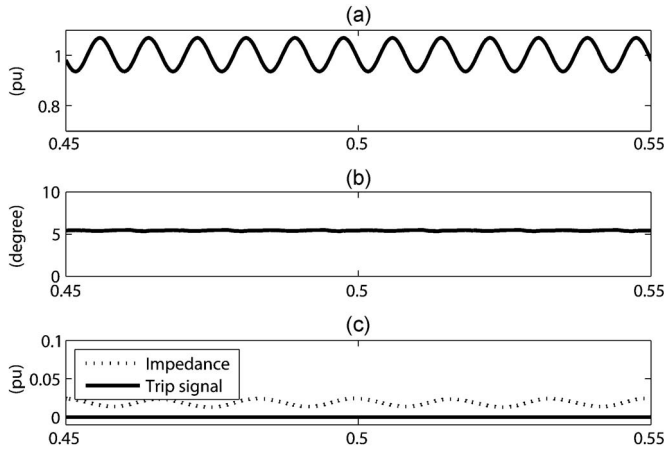

Fig. 14. Responses in case study D. (a) Magnitude of voltage. (b) Phase of voltage. (c) Variation of impedance and trip signal.

which could be detected by the other islanding detection methods because of active power mismatch.

D. Connection of Another DG System With the Same Switching Frequency Through a Transformer

As mentioned before, the proposed islanding detection technique is based on the estimation of system impedance with different switching frequencies of multiple DG systems.

In Fig. 1, the impedance of the feeders connected to the LV bus is practically small because their length is short. In contrast, the impedance of the distribution line connected to the MV bus is relatively large because its length is usually long. Therefore, as mentioned in Section II-C, the transformer and the distribution line connected to the MV bus can be modeled by using a transformer with high impedance. Then, the high-frequency harmonic components of a signal from the DG hardly pass through the modeled transformer. As a result, the same switching frequency can be used in different DG systems if they are separated from each other by a transformer. For example, the DG-1 and DG-3 systems in Fig. 1 come to this case when both DGs operate with the switching frequencies of 15 kHz. This test is carried out by the operation of Circuit breaker-3 in Fig. 1, which closes at 0.5 s.

The results are shown in Fig. 14. As with the response in case study C (see Fig. 13), the proposed method does not misjudge the change of system condition by connecting the DG-3 system as an islanding operation, even though they use the same switching frequencies in their inverters.

E. Connection of Another Load

When the load consuming a large amount of active and reactive powers is suddenly connected to the system, the conventional OUV/OUF method is subject to decide this sudden increase of load as an islanding operation because the voltage and frequency of the system change correspondingly depending on the relationships of system frequency/active power and system voltage/reactive power. In other words, the decrease in system frequency and voltage corresponds to the increase in real and reactive powers, respectively. This case is simulated

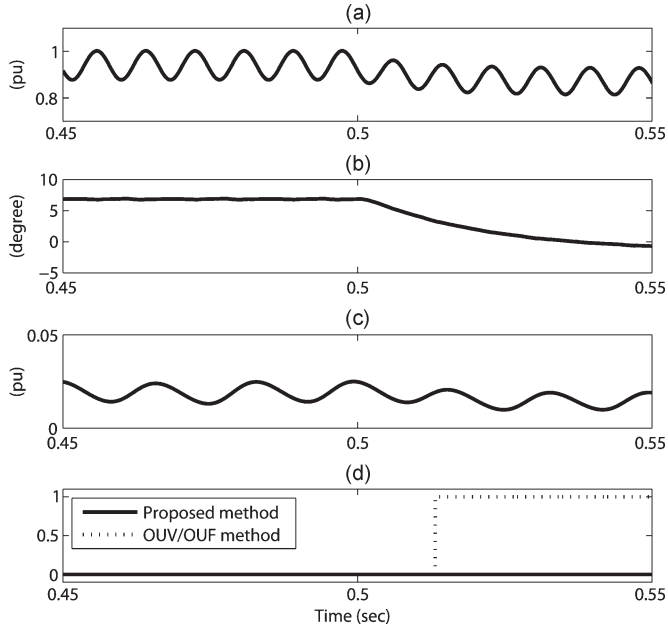

Fig. 15. Responses in case study E. (a) Magnitude of voltage. (b) Phase of voltage. (c) Variation of impedance. (d) Variation of trip signal.

by the operation of Circuit breaker-6, which closes at 0.5 s; therefore, Load-3 consuming 500 kW and 100 kVAR is suddenly connected to the system.

The results in Fig. 15(a) and (b) show that the magnitude and phase of the a-phase voltage at the terminal of DG-1 decrease after 0.5 s when Load-3 is connected. From Fig. 15(c), there exists a very small change in the variation of impedance estimated by the proposed method after 0.5 s. Therefore, it judges this change of condition correctly by not detecting it as the required islanding operation [see the result in Fig. 15(d)]. However, the OUV/OUF method erroneously detects an islanding operation.

F. Connection of Nonlinear Sensitive Load

Some nonlinear loads such as an induction motor are being practically used in industry. The induction motor drive has the special characteristic that its generated harmonic currents include all odd harmonics except for the triplen harmonics by the actions of 6- or 12-pulse rectifiers [16]. When these nonlinear sensitive loads are connected to an electric power grid, the voltage and current at the PCC connected to them are distorted. The islanding detection methods based on the THD factor can malfunction in the case with severe nonlinear sensitive loads, deteriorating power quality.

For this test, the induction motor rated at four poles, 60 Hz, and 250 kW is now connected as Load-4 at 0.5 s. At the same time, the induction motor starts operating. Then, the change in output voltage harmonics is given in Table IV. It is observed that harmonic distortions become worse for individual harmonic orders, and the corresponding value of THD also increases. Moreover, the large value of the starting current of the induction motor might cause a dip in the voltage, resulting in misjudge of islanding operation by the OUV/OUF method. These behaviors are shown in Fig. 16. However, the proposed method still operates correctly.

TABLE IV
CHANGE OF OUTPUT VOLTAGE HARMONICS IN PERCENT OF THE RATED VOLTAGE AFTER THE INDUCTION MOTOR IS CONNECTED

	Individual harmonic order					THD
	h<11	11≤h<17	17≤h<23	23≤h<35	35≤h	
Before	1.41	0.06	0.05	0.06	0.2	1.46
After	1.70	0.24	0.16	0.18	0.32	1.80

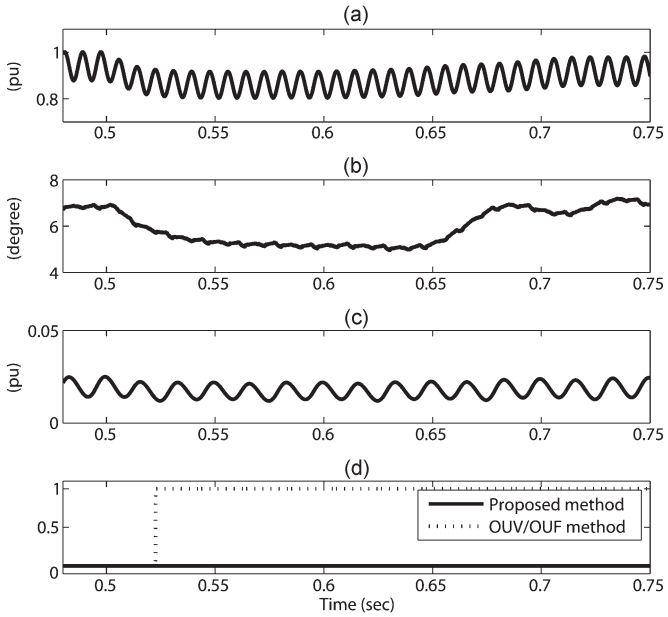

Fig. 16. Responses in case study F. (a) Magnitude of voltage. (b) Phase of voltage. (c) Variation of impedance. (d) Variation of trip signal.

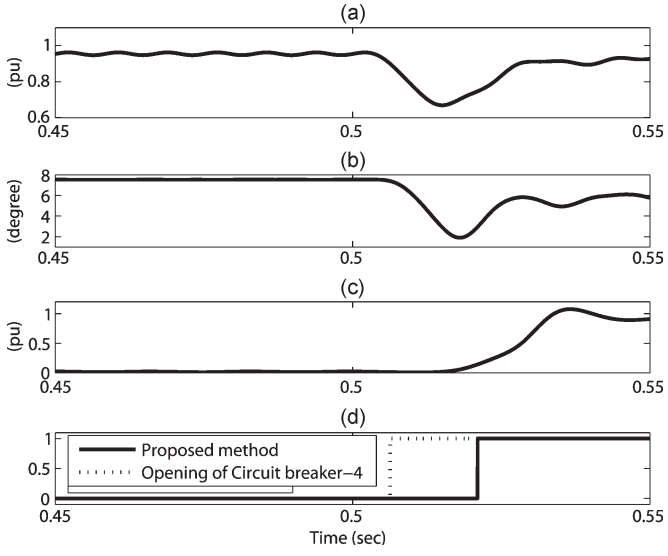

Fig. 17. Responses in case study G. (a) Magnitude of voltage. (b) Phase of voltage. (c) Variation of impedance. (d) Variation of trip signal.

G. Short-Circuit Fault Clearance

Islanding often occurs due to circuit breakers opening as part of fault clearance rather than just load distortion. For this case, a three-phase short circuit is applied to the feeder between Circuit breaker-4 and the LV bus in Fig. 1 at 0.5 s. The results in Fig. 17 show that the fault is cleared by the opening of Circuit breaker-4 at 0.5063 s in which the islanding operation of DG-1 occurs. Then, the trip signal is generated by the proposed method to open Circuit breaker-1 at 0.521 s while stopping the operation of DG-1. This proves that the proposed method correctly finds the islanding operation in the case of fault clearance within 20 ms and is therefore robust.

V. CONCLUSION

This paper has proposed a new passive islanding detection method by the estimation of system impedance based on the high switching frequency of an inverter in the DG system. The proposed method provided the zero NDZ property, which is superior to the other conventional passive methods. It is also robust in that it avoids applying the intended changes such as variations of reactive power and/or harmonics, which are required in the other active islanding detection methods. Moreover, the proposed method has been applied successfully on a distribution network with multiple grid-connected DG systems.

This study can be used as a protection algorithm when the inverter-based DG systems through several renewable energy resources are connected to an electric power grid.

REFERENCES

[1] S. I. Jang and K. H. Kim, "An islanding detection method for distributed generations using voltage unbalance and total harmonic distortion of current," *IEEE Trans. Power Del.*, vol. 19, no. 2, pp. 745–752, Apr. 2004.

[2] F. De Mango, M. Liserre, A. D. Aquila, and A. Pigazo, "Overview of anti-islanding algorithms for PV systems. Part I: Passive methods," in *Proc. IEEE Power Electron. Motion Control Conf.*, Aug. 2006, pp. 1878–1883.

[3] F. De Mango, M. Liserre, A. D. Aquila, and A. Pigazo, "Overview of anti-islanding algorithms for PV systems. Part II: Active methods," in *Proc. IEEE Power Electron. Motion Control Conf.*, Aug. 2006, pp. 1884–1889.

[4] H. H. Zeineldin, E. F. El-Saadany, and M. M. A. Salama, "Islanding detection of inverter-based distributed generation," *Proc. Inst. Elect. Eng.—Gener. Transmiss. Distrib.*, vol. 153, no. 6, pp. 644–652, Nov. 2006.

[5] Z. Ye, A. Kolwalkar, Y. Zhang, P. Du, and R. Walling, "Evaluation of anti-islanding schemes based on nondetection zone concept," *IEEE Trans. Power Electron.*, vol. 19, no. 5, pp. 1171–1175, Sep. 2004.

[6] R. A. Walling and N. W. Miller, "Distributed generation islanding-implications on power system dynamic performance," in *Proc. IEEE PES. Summer Meeting*, Jul. 2002, vol. 1, pp. 92–96.

[7] W. Freitas, W. Xu, C. M. Affonso, and Z. Huang, "Comparative analysis between ROCOF and vector surge relays for distributed generation applications," *IEEE Trans. Power Del.*, vol. 20, no. 2, pp. 1315–1324, Apr. 2005.

[8] J. B. Jeong and H. J. Kim, "Active anti-islanding method for PV system using reactive power control," *Electron. Lett.*, vol. 42, no. 17, pp. 1004–1005, Aug. 2006.

[9] R. Benato, R. Caldon, and F. Cesena, "Application of distribution line carrier-based protection to prevent DG islanding: An investigating procedure," in *Proc. IEEE Power Tech. Conf.*, Jun. 2003, vol. 3, pp. 1–7.

[10] M. Liserre, A. Pigazo, A. D. Aquila, and V. M. Moreno, "Islanding detection method for single-phase distributed generation systems based on inverters," in *Proc. IEEE Ind. Electron. Soc. Annu. Conf.*, Nov. 2005, pp. 1–6.

[11] M. Baran and F. F. Wu, "Optimal sizing of capacitors placed on a radial distribution system," *IEEE Trans. Power Del.*, vol. 4, no. 1, pp. 735–743, Jan. 1989.

[12] S. H. Lee and J. W. Park, "Selection of optimal location and size of multiple distributed generations by using Kalman-filter algorithm," *IEEE Trans. Power Syst.*, vol. 24, no. 3, pp. 1393–1400, Aug. 2009.

[13] B.-K. Choi and H.-D. Chiang, "On the local identifiability of load model parameters in measurement-base approach," *J. Elect. Eng. Technol.*, vol. 4, no. 2, pp. 149–158, Jun. 2009.

[14] S. L. Jung and Y. Y. Tzou, "Discrete sliding-mode control of a PWM inverter for sinusoidal output waveform synthesis with optimal sliding curve," *IEEE Trans. Power Electron.*, vol. 11, no. 4, pp. 567–577, Jul. 1996.
[15] J. K. Seok, S. I. Moon, S. and, and K. Sul, "Induction machine parameter identification using PWM inverter at standstill," *IEEE Trans. Energy Convers.*, vol. 12, no. 2, pp. 127–132, Jun. 1997.
[16] "Characteristics and modeling of harmonic sources-power electronic devices," *IEEE Trans. Power Del.*, vol. 16, no. 4, pp. 791–800, Oct. 2001.

Soo-Hyoung Lee (S'08) received the B.S. degree from the School of Electrical and Electronic Engineering, Yonsei University, Seoul, Korea, in 2008, where he is currently working toward the Ph.D. degree in the combined M.S. and Ph.D. program.

His research interests are in load flow of power systems, optimization of grid-connected distributed generation systems, and anti-islanding algorithms for distributed generation systems.

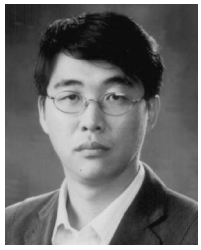

Jung-Wook Park (S'00–M'03–SM'09) received the B.S. degree (*summa cum laude*) from the Department of Electrical Engineering, Yonsei University, Seoul, Korea, in 1999, and the M.S.E.C.E. and Ph.D. degrees from the School of Electrical and Computer Engineering, Georgia Institute of Technology, Atlanta, in 2000 and 2003, respectively.

During 2003–2004, he was a Postdoctoral Research Associate in the Department of Electrical and Computer Engineering, University of Wisconsin, Madison. During 2004–2005, he was a Senior Research Engineer with LG Electronics, Inc., Seoul. He is currently an Associate Professor in the School of Electrical and Electronic Engineering, Yonsei University. His current research interests are in power system dynamics, power quality, renewable-energy-based distributed generation, optimization control algorithms, and applications of artificial neural networks.

Prof. Park was the recipient of the Second Prize Paper Award in 2003 from the Industrial Automation and Control Committee and the Prize Paper Award in 2008 from the Energy Systems Committee of the IEEE Industry Applications Society. He is currently a member of the Task Force on Intelligent Control Systems Subcommittee of the IEEE Power Engineering Society and the Vice Chair of the Intelligent Systems Applications Technical Committee of the IEEE Computational Intelligence Society. He is named in the 2006–2007 edition of *Marquis Who's Who in Science and Engineering*, the 2007–2008 edition of *Marquis Who's Who in the World*, and the 2007 inaugural edition of the International Biographical Centre's *Outstanding Scientists of the 21st Century* and *Top 100 Scientists 2007*.